

Effects of nonlinear gradient terms on the defect turbulence regime in weakly dissipative systemsJ. B. Gonpe Tafo,^{1,2,*} L. Nana,^{1,†} and T. C. Kofane^{2,3,‡}¹*Laboratoire de Physique Fondamentale, Groupe Phénomènes Non Linéaires et Systèmes Complexes, UFD de Mathématique, Informatique Appliquée et Physique Fondamentale, Université de Douala, Boîte Postale 24157, Douala, Cameroon*²*Centre d'Excellence Africain en Technologies de l'Information et de la Communication, Boîte Postale 812, Yaoundé, Cameroon*³*Laboratoire de Mécanique, Département de Physique, Faculté des Sciences, Université de Yaoundé I, Boîte Postale 812, Yaoundé, Cameroon*

(Received 24 April 2017; published 9 August 2017)

We investigate the behavior of traveling waves in a defect turbulence regime with the periodic boundary conditions by using the lowest-order complex Ginzburg-Landau equation (CGLE), and we show the effect of the nonlinear gradient terms in the system. It is found that the nonlinear gradient terms which appear at the same order as the quintic term can change the behavior of the wave patterns. The presence of the nonlinear gradient terms can cause major changes in the behavior of the solution. They can be considered like the stabilizing terms. The system which was initially unstable or chaotic can become stable by including the nonlinear gradient terms.

DOI: [10.1103/PhysRevE.96.022205](https://doi.org/10.1103/PhysRevE.96.022205)**I. INTRODUCTION**

New theoretical approaches, experimental analyses, and systematic use of computer science in data processing have been developed during the past 20 years in the context of pattern-forming nonequilibrium systems including fields such as quantum optics, hydrodynamic instabilities, autocatalytic chemical reactions, and nonlinear oscillators in diverse fields. These give a useful framework of reference to discuss the formation, selection, and stability properties of nonlinear and nonequilibrium phenomena [1,2]. For example, it has become quite clear that hydrodynamic instabilities manifest themselves in the form of various patterns which vary from the simple to the complex. Hence a few relatively simple systems, such as Rayleigh-Bénard, Taylor-Couette, and Bénard-Marangoni systems, became very popular as prototypes that reveal a rich variety of complicated behavior in space and time, which can have both coherent and chaotic components, where nonlinear theories of dissipative pattern formation in nonequilibrium systems may easily be tested [1,2].

To model those driven nonlinear systems with dissipation and dispersion, some prototype of nonlinear evolution equations has been derived using three approaches. The first class of prototype equations which describe correctly the dynamics of the system on long space-time scales near the onset of the instability is amplitude or envelope equations, which describe the slowly varying amplitude of a plane wave, and for which the distance from onset is the expansion parameter. An example is the cubic complex Ginzburg-Landau (CGL) equation, which arises as an envelope equation near a forward bifurcation to traveling waves [3–6]. The other example is the cubic-quintic CGL equation, which arises near the onset of a weakly inverted bifurcation associated with traveling waves [7–9]. The second class of prototype equations for the investigations of pattern-formation problems can be understood quantitatively in terms of theoretical models involving nonlinear phase equations, which describe the slowly varying phase of a plane wave and

thus provide a welcome test of this theoretical approach well above the bifurcation where amplitude equations are no longer applicable. The prototype of a nonlinear phase equation is the Kuramoto-Sivashinsky equation [10,11]. Sometimes, there is coupling between amplitude and phase equations. The third class of prototype equations is order parameter equations, which contain a phenomenological aspect, and whose use in the field of pattern formation was pioneered by Swift and Hohenberg [12]. They are constructed such that they reduce to the appropriate envelope equation near the onset of the instability and also reflect the correct symmetry of the underlying problem.

The cubic and the cubic-quintic CGL equations play an important role in many branches of physics, such as Taylor-Couette flow [13–15], Rayleigh-Bénard convection [3,4], plan Poiseuille flow in fluid systems [16], chemical disturbances [17], ionization waves in the glow discharge [18], nonlinear optics [19–23], laser physics [24–29], theory of phase transitions [30], nonlinear transmission line [31–35], stick-slip motion [36], Bose-Einstein condensates [37], liquid-gas interfaces [38], ferromagnets [39,40], and DNA molecular systems [41]. The one-dimensional cubic and the cubic-quintic CGL equations possess a rich variety of solutions including coherent structures such as pulses (solitary waves), fronts (shock waves), sinks (propagating hole with asymptotic group velocity negative), sources (propagating hole with asymptotic group velocity positive), periodic unbounded solution [42–51], vacuum, periodic and quasiperiodic solutions [52], slowly varying fully nonlinear wave trains [53], and a transition to chaos [54–61].

In many applications, there are many ways to generalize the above amplitude, phase, and order parameter equations, in order to include qualitatively new features, such as higher-order derivatives, higher-order nonlinearities, differential operators, symmetry groups, and nonlinear gradient terms, and the resulting evolution equations are considerably more complicated than the original evolution equations. An interesting example which contains additional nonlinear gradient terms is the one-dimensional lower-order complex Ginzburg-Landau (LOCGL) equation [62–65]. The LOCGL equation which describes a system exhibiting a subcritical bifurcation to traveling waves must contain a quintic nonlinearity. At this

*Corresponding author: joelgbruno@yahoo.fr

†la_nanad@yahoo.fr

‡tckofane@yahoo.com

order, it is necessary to include the lower-order nonlinear gradient terms:

$$\begin{aligned}
 A_t + VA_x = & (\chi_r + i\chi_i)A + (1 + ic_1)A_{xx} + (1 - ic_3)|A|^2A \\
 & - (1 - ic_5)|A|^4A - q_1|A|^2A_x \\
 & - q_2|A|_x^2A - q_3A^2A_x^*, \quad (1)
 \end{aligned}$$

with $q_1 = q_{1r} + iq_{1i}$, $q_2 = q_{2r} + iq_{2i}$, and $q_3 = q_{3r} + iq_{3i}$. Here $A(x, t)$ describes the amplitude of extended spatial patterns. The value c_1 is associated with spatial dispersion, while c_3 and c_5 are associated with nonlinear dispersions. V is the linear group velocity of the waves. The values q_1 , q_2 , and q_3 represent coefficients of nonlinear gradient terms. It has been shown that the nonlinear gradient terms cause an asymmetry on localized states and change the value and even the sign of the group velocity with which the localized states propagate. For large enough values of the nonlinear gradient terms the localized states become unstable [62–64]. Two of these nonlinear gradient terms, i.e., $|A|^2A_x$ and $A^2A_x^*$ appear naturally in the asymptotic derivation. A sufficient condition, $|q_{1i} - q_{3i}| < 2$, has been proven for the global existence of solutions to the Cauchy problem of this equation [66,67]. However, it has been observed that restricted classes of bounded solutions including traveling waves may exist outside this parameter range. The last term $|A|_x^2A$ is a local term that has been introduced to stabilize the solutions of variable size. This last nonlinear gradient term has significant consequences on the width of the localized solutions and provides a good model for the description of turbulent patches in laminar domains [68]. In addition, in Refs. [69,70] the author also focused his work in particular on the effect of the gradient term $|A|_x^2A$, which expresses the advection of the concentration field by the traveling wave. As shown by Barten *et al.* [71,72] the wave generates a concentration current which is antisymmetric with respect to the midplane of the convection layer.

Since we take the periodic boundary conditions, the convective term VA_x may be transformed away by going into a moving frame of reference. Also, the parameter $\chi = \chi_r + i\chi_i$, which is proportional to the distance from criticality, can be taken as real, since the imaginary part can be transformed away by a simple transformation [73].

The present study extends our previous research into the spatiotemporal dynamics observed in Fig. 1 by adding the nonlinear terms to the system. We have chosen to associate the three nonlinear gradient terms in order to study their impact in a defect turbulence regime. The effects of the nonlinear gradient terms are examined by using the indicators such as the Lyapunov exponent and the energy bifurcation diagram.

The outline of this paper is as follows: in Sec. II, we give an analytical approach of the model equation in order to determine the new Benjamin-Feir-Newell condition. In Sec. III, we detail the effects of the nonlinear gradient terms on the spatiotemporal dynamics of nonlinear traveling waves. Finally, concluding remarks are made in Sec. IV.

II. ANALYTICAL STUDY

In this study, we determine the growth rate λ , of which the nature of the system (stability or instability) depends on its

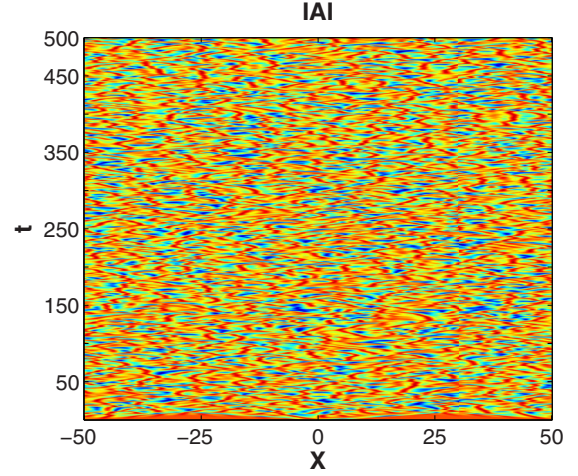


FIG. 1. Defect turbulence regime observed for $\chi = 0.6$, $c_1 = 2.5$, $c_3 = 0.5$, $c_5 = 1.1$, and $L = 150$, with $q_1 = q_2 = q_3 = 0.0 + 0.0i$.

sign. We determine also the Benjamin-Feir Newell condition in the case of the LOCGL equation.

In order to investigate how weak and time-dependent perturbations evolve along the extended system described by the LOCGL equation, we consider the following linear-stability analysis. Equation (1) admits the trivial solution $A = 0$ and spatially homogeneous solutions of finite amplitude:

$$A = A_0 e^{i\omega t}, \quad \text{where } |A_0|^2 = \frac{1}{2}(1 \pm \sqrt{1 + 4\chi_r}), \quad (2)$$

with $\omega = -|A_0|^4(c_3 - c_5|A_0|^2)$. The existence of A_0 requires that $\chi_r \geq \frac{-1}{4}$ for a subcritical bifurcation. The linear stability of the steady state can be examined by introducing a perturbed field of the following form:

$$A(x, t) = A_0 e^{i\omega t} [1 + \varepsilon B(x, t)], \quad (3)$$

where $\varepsilon \ll 1$. Substituting solution (3) into Eq. (1), we obtain upon linearization the equation for the perturbed field as follows:

$$\begin{aligned}
 B_t + i\omega B = & \chi_r B + (1 + ic_1)B_{xx} \\
 & + B|A_0|^2[2(1 - ic_3) - 3(1 - ic_5)|A_0|^2] \\
 & + |A_0|^2 B^*[(1 - ic_3) - 2(1 - ic_5)|A_0|^2] \\
 & - |A_0|^2 B_x[(q_{1r} + q_{2r}) + i(q_{1i} + q_{2i})] \\
 & - |A_0| B_x^*[(q_{2r} + q_{3r}) + i(q_{2i} + q_{3i})]. \quad (4)
 \end{aligned}$$

The symbol $*$ denotes a complex conjugate. We assume a general solution of the following form:

$$B = B_1(t)e^{ikx} + B_2(t)e^{-ikx}, \quad (5)$$

where k represents the wave number. One gets a closed system of equations for $B_1(t)$ and $B_2^*(t)$, setting $B_1(t) \propto B_{10}e^{\lambda t}$ and $B_2(t) \propto B_{20}e^{\lambda t}$. After substituting Eq. (5) into Eq. (4), we obtain the determinant

$$\begin{vmatrix} (a - b) - i(c + d) & (e + f) - i(g + h) \\ (e - f) + i(g - h) & (a + b) + i(c - d) \end{vmatrix} = 0, \quad (6)$$

where

$$\begin{aligned} a &= \chi_r - k^2 + |A_0|^2(2 - |A_0|^2) - \lambda, \\ b &= k|A_0|^2(q_{1i} + q_{2i}), \\ d &= k|A_0|^2(q_{1r} + q_{2r}), \\ c &= \omega + k^2c_1 + |A_0|^2(2c_3 - 3c_5|A_0|^2), \\ e &= |A_0|^2(1 - 2|A_0|^2), \end{aligned} \quad (7)$$

and

$$\begin{aligned} f &= k|A_0|^2(q_{2i} + q_{3i}), \\ g &= k|A_0|^2(c_3 - 2c_5|A_0|^2), \\ h &= k|A_0|^2(q_{2r} + q_{3r}). \end{aligned} \quad (8)$$

We arrive at the following nonlinear dispersion relation $\lambda(k, |A_0|^2)$:

$$\lambda_{+,-} = -[k^2 - \chi_r + |A_0|^2(2 - 3|A_0|^2)] \pm \sqrt{M - N}, \quad (9)$$

where

$$\begin{aligned} M &= |A_0|^4[(1 - 2|A_0|^2)^2 + k^2\{(q_{2r} + q_{1r})^2 + (q_{2i} + q_{1i})^2 \\ &\quad - (q_{2r} + q_{3r})^2 + (q_{2i} + q_{3i})^2\} + (c_3 - 2c_5|A_0|^2)^2], \end{aligned}$$

and

$$N = [\omega + c_1k^2 + |A_0|^2(2c_3 - 3c_5|A_0|^2)]. \quad (10)$$

The negative sign ($-$) of the square root in Eq. (9) corresponds to amplitude modes, while the positive sign ($+$) is for the phase modes [61]. In the last case, for very large k , the growth rate is negative and behaves as $-k^2$. So, short wavelength perturbations are always damped. However, long wavelength perturbations can grow, destabilizing the original plane-wave solution. By replacing χ_r and ω in Eq. (9) with the values given by Eq. (2), we expand it for small k :

$$\lambda_{\pm} = Pk^2 + O(k^4), \quad (11)$$

where

$$P = -\frac{u + v}{-1 + 2|A_0|^2}, \quad (12)$$

with

$$\begin{aligned} u &= -1 + 2|A_0|^2 - c_1(-c_3 + 2c_5|A_0|^2) \\ &\quad + |A_0|^2(q_{1i}^2 - q_{3i}^2 - q_{3r}^2), \\ v &= 2|A_0|^2(q_{2i}q_{3i} + q_{2r}q_{3r} - q_{2i}q_{1i} - q_{1r}q_{2r}). \end{aligned} \quad (13)$$

If the coefficient P is negative, the system remains stable. The criterion of the instability is given by

$$u + v < 0. \quad (14)$$

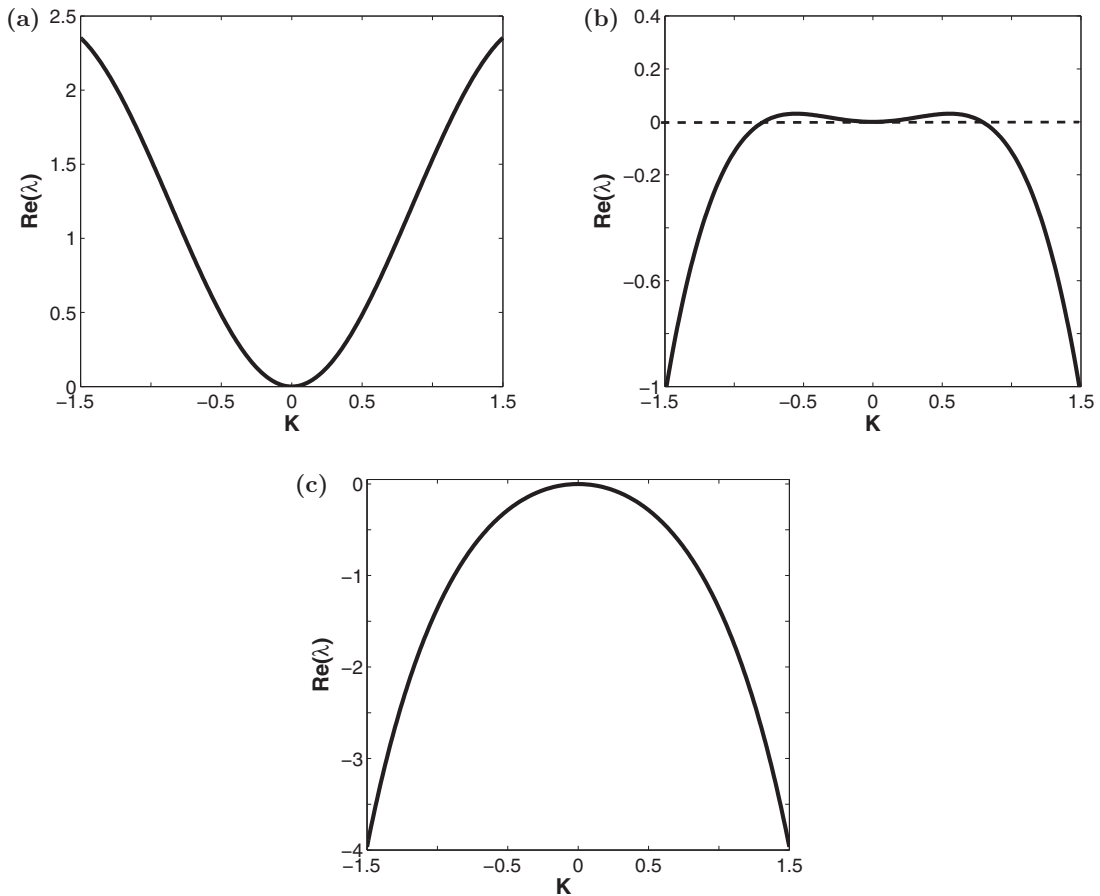


FIG. 2. Variation of (k, λ) for $\chi = 0.6$, $c_1 = 2.5$, $c_3 = 0.5$, $c_5 = 1.1$, and $L = 150$, with (a) $q_1 = q_2 = q_3 = 0.0 + 0.0i$, (b) $q_1 = 0.1 + 0.1i$ and $q_2 = q_3 = 0.4 + 0.4i$, and (c) $q_1 = 0.5 + 0.5i$ and $q_2 = q_3 = 1.0 + 1.0i$.

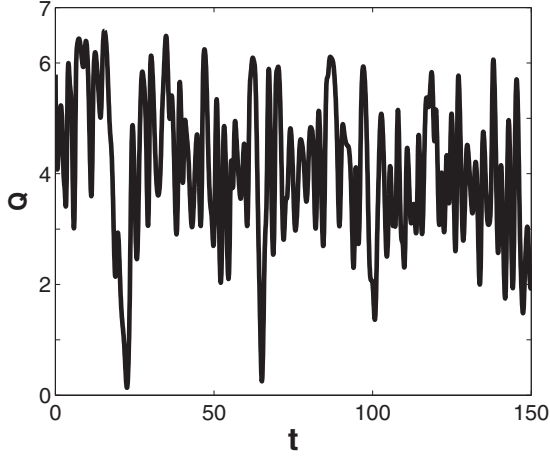


FIG. 3. Localized pattern energy Q in defect turbulence regime with $q_1 = q_2 = q_3 = 0.0 + 0.0i$.

This condition represents the criterion of Benjamin-Feir-Newell in the LOCGL equation. Let us remark that if the nonlinear terms are suppressed, we have the usual criterion of

the Benjamin-Feir-Newell in the cubic-quintic case given by $1 - c_1c_3 - 2|A_0|^2(1 - c_1c_5) > 0$ [61].

In Fig. 2, we plot the (k, λ_+) curves for different values of the nonlinear gradient terms. When the nonlinear gradient values are zero, the system is completely unstable [Fig. 2(a)]. It is obvious that, as the nonlinear gradient terms increase, the instability region is replaced by the stable region and the system becomes more and more stable [Figs. 2(b) and 2(c)].

III. NUMERICAL SIMULATIONS

In this section, we introduce some definitions, equations, and numerical algorithms that are used in order to obtain useful results that are discussed below.

A. Dynamical indicators

We essentially characterize the different types of dynamical behavior of the system by the energy function Q and the largest Lyapunov exponent λ_{\max} . The first one is defined by

$$Q(t) = \frac{1}{2L} \int_{-L}^L |A(x,t)|^2 dx, \quad (15)$$

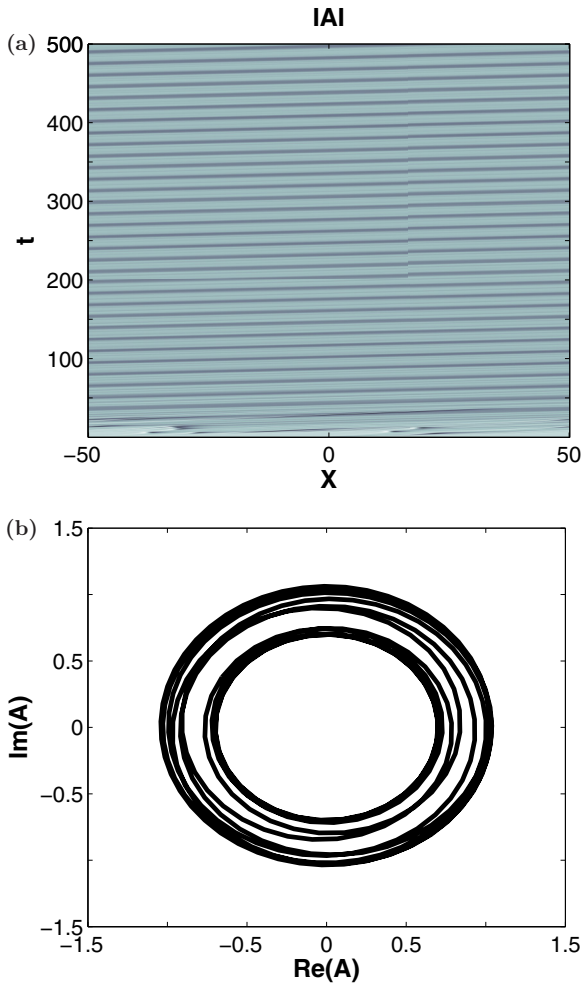


FIG. 4. (a) Running wave regime for $\chi = 0.6$, $q_1 = 0.5 + 0.9i$, $q_2 = 0.6 + 0.6i$, and $q_3 = 0.9 + 0.9i$. (b) Phase portrait of running waves.

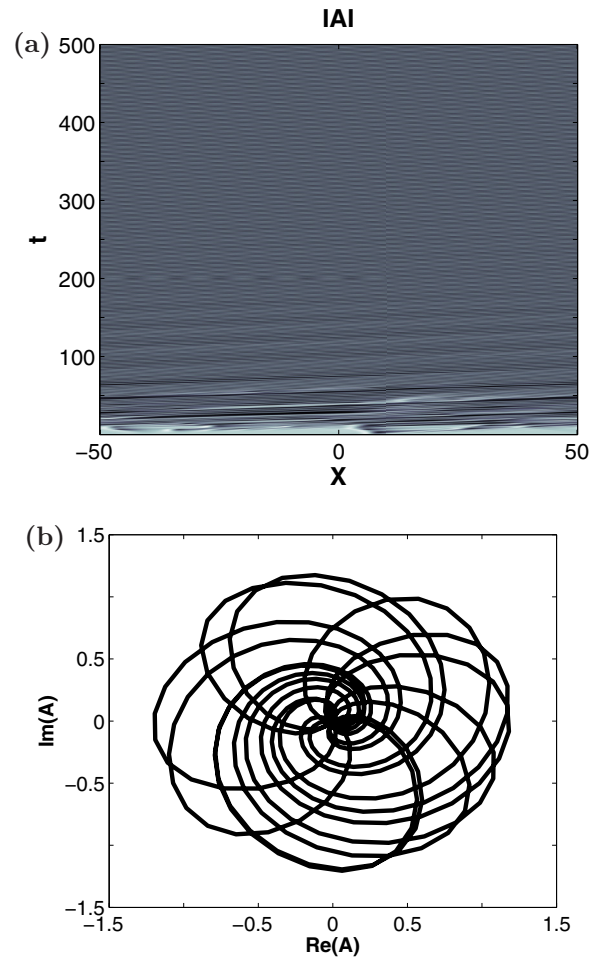


FIG. 5. Oscillating regime in system for $\chi = 0.6$, $q_1 = 1.5 + 0.5i$, $q_2 = 0.6 + 0.6i$, and $q_3 = 1.5 + 0.9i$. (a) Space-time plot of $|A|$ propagating in one dimension. (b) Phase portrait of wave patterns.

which is frequently used to characterize nonregular dynamics in optics [74], localized patterns in fluids, and other physical systems [75]. The one-dimensional system is assumed to be of length $2L$. In order to check more of the dynamic behavior of the system and to provide a more quantitative aspect of the dynamics, we calculate the largest Lyapunov exponent defined by [76,77]

$$\lambda_{\max} = \lim_{t \rightarrow \infty} \left[\frac{1}{t} \ln \left(\frac{\|\delta A(x,t)\|}{\|\delta A(x,0)\|} \right) \right], \quad \text{with}$$

$$\|\delta A(x,t)\| = \left\{ \int_{x=-L}^{x=L} |\delta A(x,t)|^2 dx \right\}^{1/2}, \quad (16)$$

where δA is a small perturbation such as $A = A_0 + \delta A$, A_0 is the initial value of the amplitude wave. Here, $\delta A(x,0) = 10^{-4}A_0$, and δA satisfies the linearized evolution equation

$$\frac{\partial \delta A}{\partial t} = \bar{\mathbf{J}} \cdot \delta A, \quad (17)$$

with $\bar{\mathbf{J}}$ being the Jacobian matrix of Eq. (1). This number quantifies how fast the distance between two initially close trajectories δA of the vector field A either vanishes exponentially ($\lambda_{\max} < 0$) or diverges ($\lambda_{\max} > 0$). The largest Lyapunov exponent is the dynamical invariant most easily and

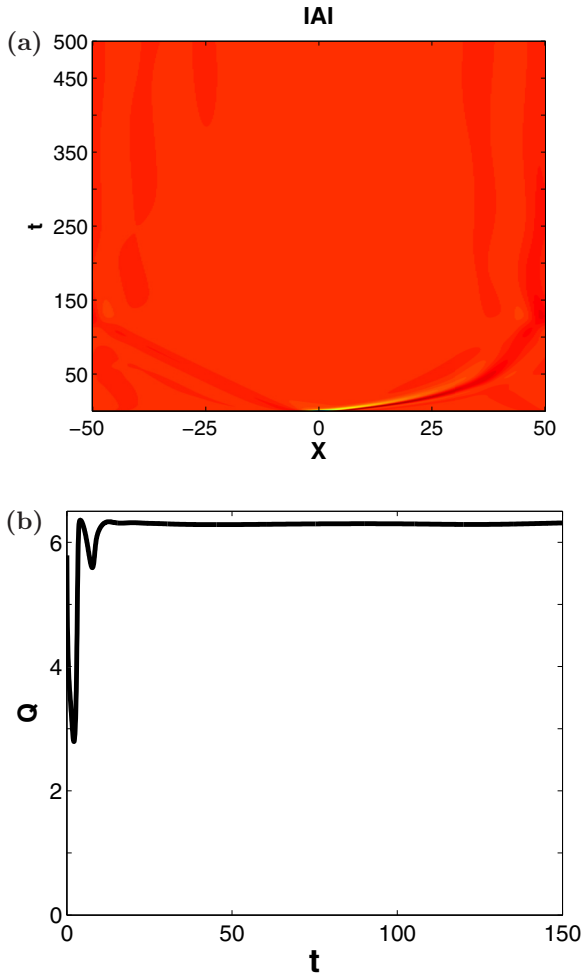


FIG. 6. (a) Laminar regime and (b) pattern energy Q , as a function of time for $q_1 = 1.5 + 0.5i$ and $q_2 = q_3 = 1.5 + 1.5i$.

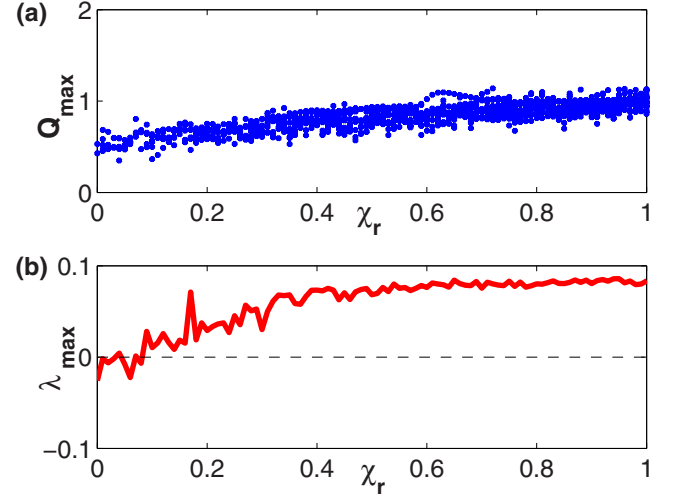


FIG. 7. (a) Bifurcation diagram of Q_{\max} and (b) largest Lyapunov exponent λ_{\max} as a function of χ_r , without nonlinear gradient terms.

accurately estimated from the experimental time series [77]. This method has been extensively used for many different dynamical systems to quantify chaos [78–82].

In fact, when λ_{\max} is positive or negative, the perturbation of a given trajectory is characterized by an exponential separation or approach, respectively. Hence, attractors such as stationary patterns or uniform equilibria are characterized by negative λ_{\max} . Conversely, complex behaviors such as chaos and spatiotemporal chaos will exhibit positive λ_{\max} . Dynamical behaviors whose the largest Lyapunov exponent is zero correspond to equilibria with invariant directions, such as periodic or quasiperiodic solutions and nonchaotic attractors characterized with polynomial growth rate [79].

B. Numerical results

To solve numerically Eq. (1), we use a finite difference scheme in space and the standard fourth-order Runge-Kutta

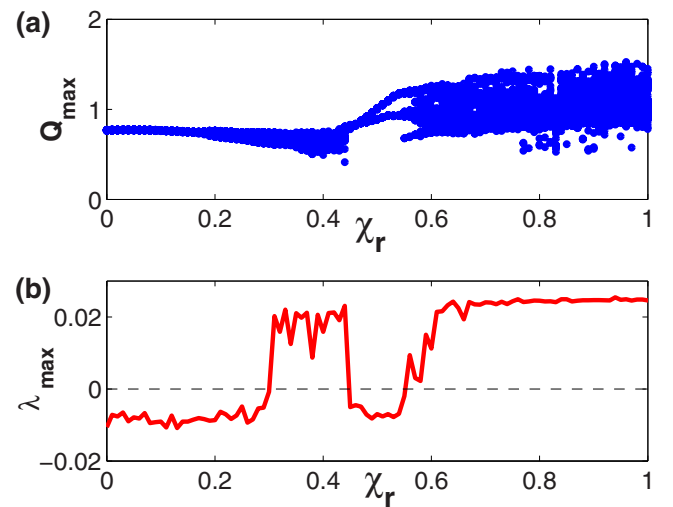


FIG. 8. (a) Bifurcation diagram of Q_{\max} and (b) largest Lyapunov exponent λ_{\max} as a function of χ_r , with $q_1 = 0.1 + 0.1i$, $q_2 = 0.2 + 0.2i$, and $q_3 = 0.3 + 0.3i$.

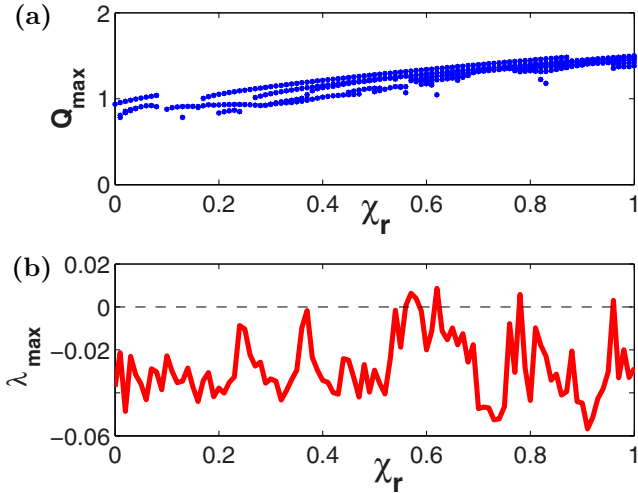


FIG. 9. (a) Bifurcation diagram of Q_{\max} and (b) largest Lyapunov exponent λ_{\max} as a function of χ_r , with $q_1 = 0.8 + 0.8i$, $q_2 = 0.5 + 0.5i$, and $q_3 = 0.7 + 0.7i$.

algorithm in time [61,83]. The numeric results' precision is examined by testing several steps of integration in space and in time. We have chosen a grid spacing of $dx = 0.25$ and the typical time step was $dt = 0.01$. The parameters c_1 , c_3 , and c_5 were taken in a defect turbulence region [61]. The precise nature of the observed dynamics in the system depends sensitively on the choice of the nonlinear gradient terms' values. The main results are given in Figs. 3–10. In particular, we concentrate the discussion on the influence of the nonlinear gradient terms. Figure 3 shows the energy as a function of time corresponding to the defect turbulence regime. It confirms the chaotic behaviors of the system with fluctuations which can be observed. By taking into account the presence of the nonlinear gradient terms, the dynamics of the system changes. Oscillating patterns are observed in the domain as is seen in Figs. 4 and 5; the corresponding largest Lyapunov exponent is zero. Figure 4 shows the presence of the running waves into the system [84,85]. There are quasiperiodic states. The motion of waves travel at constant speed and take one direction, according to their initial condition, and this is the so-called oriental symmetry breaking. A double periodicity

in time and in space is observed. In Fig. 5, we have another type of oscillating pattern in a color-coded space-time plot [see Fig. 5(a)]. After a transient time, the waves propagate uniformly, with a well-defined wave number and constant amplitude. We note also the presence of an attractor into the system which annihilates the wave patterns [Fig. 5(b)].

With the values q_1 , q_2 , and q_3 getting larger and larger, the system is completely stable [see Fig. 6(a)]. The corresponding energy function observed in Figure 6(b) shows the constant value of Q_{\max} whatever the value of χ_r , which confirms the stability of the system. The drop observed near $x = 0$ expresses the fact that the initial condition is a hole.

Figures 7–9 show the largest Lyapunov exponent λ_{\max} and the bifurcation diagram of the pattern state as a function of the control parameter χ_r for Eq. (1). They allow us to see clearly how the system changes its dynamical behavior with the presence of the nonlinear gradient terms.

Figure 7(a), which expresses the case without the nonlinear gradient terms, is obtained by taking repeatedly the maximum value of the energy function Q_{\max} in a given time interval at different times (well after the transient is died); this is done for many different values of the control parameter χ_r . As can be seen, the system is briefly stable, and then the instability is present in the whole system. In fact, if there is a unique Q_{\max} , then the system is stationary or periodic, while for finite continuous distribution of Q_{\max} values, the behavior is either quasiperiodic or chaotic.

The Lyapunov exponent shown in Fig. 7(b) indicates the dynamical behavior of the system and confirms the results. Figure 8 is obtained for increasing values of the nonlinear gradient terms. We observe several transitions between regular and chaotic states. In particular, there is a small stability part of the system in the range $\chi_r \in (0.0, 0.3)$. Beyond the point $\chi_r = 0.44$, the system becomes stable again until the value $\chi_r = 0.55$, with another bifurcation point at $\chi_r = 0.6$. On the other hand, the transition from a regular to a chaotic wave pattern is flat. In the plot of the Lyapunov exponent [Fig. 8(b)], the chaotic motions identified are validated by the positive values of λ_{\max} , while the stable region corresponds to the negative values of λ_{\max} . For the large value of the nonlinear gradient terms, the system becomes more and more stable as is seen in Fig. 9. The phase space trajectory seen in Fig. 10 illustrates the dynamic behaviors which are visualized at different points

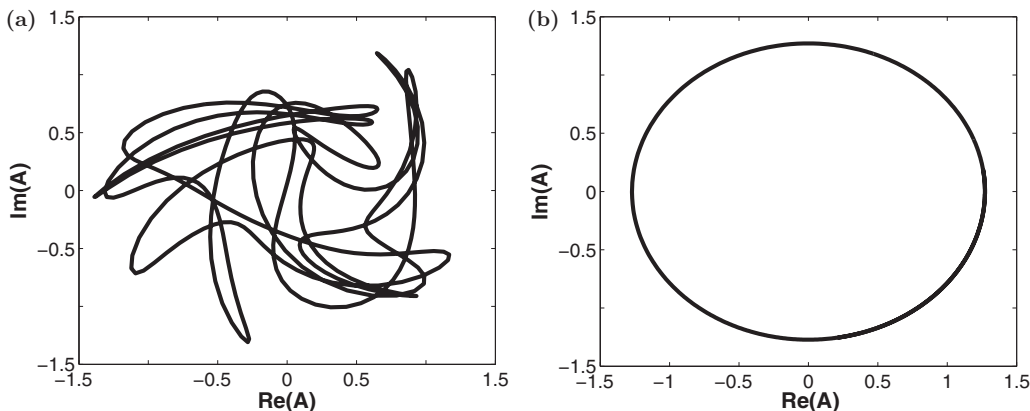


FIG. 10. Phase portrait of Fig. 7 showing (a) the chaotic case and (b) the stationary case.

of the bifurcation diagram of Fig. 8(a). For the value $\chi_r = 0.8$ in the unstable region, the chaotic motion is obvious as is seen in Fig. 10(a). The amplitude of the variable accidentally drops to zero to produce defects. The phase space of Fig. 10(b) obtained in the stable region shows that all the chaotic motions are suppressed, and a stationary state is observed.

IV. CONCLUSION

In this paper, we have studied the effects of nonlinear gradient terms on dissipative systems by using the lowest-order Ginzburg-Landau equation. First of all, we have calculated

analytically the parameter regions where wave amplitude can be stabilized by establishing the new criterion of Benjamin-Feir-Newell (BFN) for the lowest-order Ginzburg-Landau equation. We have found that this criterion is not similar to the one obtained in the cubic-quintic Ginzburg-Landau equation case.

By considering the wave patterns in the chaotic regions in particular in a defect turbulence, it was shown that the presence of the nonlinear gradient terms changes the dynamical behavior of the system: the chaos disappears progressively in the domain. The fact that the nonlinear gradient terms can stabilize the system leads us to conclude that they can be considered as the stabilizing terms.

-
- [1] M. C. Cross and P. C. Hohenberg, *Rev. Mod. Phys.* **65**, 851 (1993).
- [2] I. Aranson and L. Kramer, *Rev. Mod. Phys.* **74**, 99 (2002).
- [3] A. C. Newell and J. A. Whitehead, *J. Fluid Mech.* **38**, 279 (1969).
- [4] L. A. Segel, *J. Fluid Mech.* **38**, 203 (1969).
- [5] H. R. Brand, P. S. Lomdahl, and A. C. Newell, *Phys. Lett. A* **118**, 67 (1986).
- [6] H. R. Brand, P. S. Lomdahl, and A. C. Newell, *Phys. D (Amsterdam, Neth.)* **23**, 345 (1986).
- [7] O. Thual and S. Fauve, *J. Phys. (France)* **49**, 1829 (1988).
- [8] R. J. Deissler and H. R. Brand, *Phys. Rev. Lett.* **72**, 478 (1994).
- [9] O. Descalzi and H. R. Brand, *Phys. Rev. E* **72**, 055202(R) (2005).
- [10] Y. Kuramoto and T. Tsuzuki, *Prog. Theor. Phys.* **54**, 687 (1975).
- [11] G. Sivashinsky, *Acta Astronaut.* **4**, 1177 (1977).
- [12] J. Swift and P. C. Hohenberg, *Phys. Rev. A* **15**, 319 (1977).
- [13] A. S. Kogelman and R. C. Di Prima, *Phys. Fluids* **13**, 1 (1970).
- [14] J. T. Stuart and R. C. Di Prima, *Proc. R. Soc. London, Ser. A* **362**, 27 (1978).
- [15] A. Recktenwald, M. Lücke, and H. W. Müller, *Phys. Rev. E* **48**, 4444 (1993).
- [16] K. Stewartson and J. T. Stuart, *J. Fluid Mech.* **48**, 529 (1971).
- [17] Y. Kuramoto and T. Yamada, *Prog. Theor. Phys.* **56**, 679 (1976).
- [18] N. Bekki, *J. Phys. Soc. Jpn.* **50**, 659 (1981).
- [19] C. Pare, L. Gagnon, and P. A. Belanger, *Opt. Commun.* **74**, 228 (1989).
- [20] P. A. Belanger, L. Gagnon, and C. Pare, *Opt. Lett.* **14**, 943 (1989).
- [21] G. P. Agrawal, *Phys. Rev. A* **44**, 7493 (1991).
- [22] C. J. Chen, P. K. A. Wai, and C. R. Menyuk, *Opt. Lett.* **19**, 198 (1994).
- [23] R. Conte and M. Musette, *Pure Appl. Opt.* **4**, 315 (1995).
- [24] R. Graham and H. Haken, *Z. Phys.* **213**, 420 (1968).
- [25] R. Graham and H. Haken, *Z. Phys.* **237**, 31 (1970).
- [26] P. K. Jakobsen, J. V. Maloney, A. C. Newell, and R. Indik, *Phys. Rev. A* **45**, 8129 (1992).
- [27] G. K. Harkness, W. J. Firth, J. B. Geddes, J. V. Moloney, and E. M. Wright, *Phys. Rev. A* **50**, 4310 (1994).
- [28] L. Gil, *Phys. Rev. Lett.* **70**, 162 (1993).
- [29] M. San Miguel, *Phys. Rev. Lett.* **75**, 425 (1995).
- [30] R. Graham, in *Fluctuations, Instabilities and Phase Transitions*, edited by T. Riste (Springer, Berlin, 1975).
- [31] F. B. Pelap, T. C. Kofane, N. Flytzanis, and M. Remoissenet, *J. Phys. Soc. Jpn.* **70**, 2568 (2001).
- [32] D. Yemele, P. K. Talla, and T. C. Kofane, *J. Phys. D: Appl. Phys.* **36**, 1429 (2003).
- [33] E. Kengne and Kum K. Cletus, *Int. J. Mod. Phys. B* **19**, 3961 (2005).
- [34] F. II. Ndzana, A. Mohamadou, T. C. Kofane, and L. Q. English, *Phys. Rev. E* **78**, 016606 (2008).
- [35] F. II Ndzana, A. Mohamadou, and T. C. Kofane, *Phys. Rev. E* **79**, 056611 (2009).
- [36] O. Hirayama, K. Ohtsuka, S. Ishiwata, and S. Watanabe, *Phys. D (Amsterdam, Neth.)* **185**, 97 (2003).
- [37] F. T. Arecchi, J. Bragard, and L. M. Castellano, *Opt. Commun.* **179**, 149 (2000).
- [38] K. Zakaria and Y. Gamiel, *Int. J. Nonlinear Mechanics* **47**, 951 (2012).
- [39] A. Zubrzycki, *J. Magn. Magn. Mater.* **150**, L143 (1995).
- [40] J. P. Nguenang, T. Njassap, and T. C. Kofane, *Eur. Phys. J. B* **65**, 539 (2008).
- [41] C. B. Tabi, A. Mohamadou, and T. C. Kofane, *Chin. Phys. Lett.* **26**, 068703 (2009).
- [42] L. M. Hocking and K. Stewartson, *Proc. R. Soc. London, Ser. A* **326**, 289 (1972).
- [43] N. R. Pereira and L. Stenflo, *Phys. Fluids* **20**, 1733 (1977).
- [44] K. Nozaki and N. Bekki, *J. Phys. Soc. Jpn.* **53**, 1581 (1984).
- [45] N. Bekki and K. Nozaki, *Phys. Lett. A* **110**, 133 (1985).
- [46] F. Cariello and M. Tabor, *Phys. D* **39**, 77 (1989).
- [47] R. Conte and M. Musette, *Phys. D (Amsterdam, Neth.)* **69**, 1 (1993).
- [48] W. van Saarloos and P. C. Hohenberg, *Phys. Rev. Lett.* **64**, 749 (1990).
- [49] A. Mohamadou, A. K. Jiotsa, and T. C. Kofané, *Phys. Rev. E* **72**, 036220 (2005).
- [50] A. Mohamadou and T. C. Kofane, *Phys. Rev. E* **73**, 046607 (2006).
- [51] N. Akhmediev, J. M. Soto-Crespo, and G. Town, *Phys. Rev. E* **63**, 056602 (2001).
- [52] T. Kapitula, *Nonlinearity* **9**, 669 (1996).
- [53] A. J. Bernoff, *Phys. D (Amsterdam, Neth.)* **30**, 363 (1988).
- [54] B. P. Luce, *Phys. D (Amsterdam, Neth.)* **84**, 553 (1995).
- [55] H. Chate, *Phys. D (Amsterdam, Neth.)* **86**, 238 (1995).
- [56] P. Kolodner, S. Slimani, N. Aubry, and R. Lima, *Phys. D (Amsterdam, Neth.)* **85**, 165 (1995).
- [57] M. Bazhenov, M. Rabinovich, and L. Rubchinsky, *J. Stat. Phys.* **83**, 1165 (1996).

- [58] K. Nozaki and N. Bekki, *Phys. Rev. Lett.* **51**, 2171 (1983).
- [59] A. K. Jiotsa and T. C. Kofane, *J. Phys. Soc. Jpn.* **72**, 1800 (2003).
- [60] J. B. Gonpe Tafo, L. Nana, and T. C. Kofane, *Phys. Rev. E* **88**, 032911 (2013).
- [61] J. B. Gonpe Tafo, L. Nana, and T. C. Kofane, *Eur. Phys. J. Plus* **126**, 105 (2011).
- [62] H. R. Brand and R. J. Deissler, *Phys. Rev. Lett.* **63**, 2801 (1989).
- [63] R. J. Deissler and H. R. Brand, *Phys. Lett. A* **146**, 252 (1990).
- [64] R. J. Deissler and H. R. Brand, *Phys. Rev. Lett. A* **81**, 3856 (1998).
- [65] E. Yomba and T. C. Kofane, *J. Phys. Soc. Jpn.* **69**, 1027 (2000).
- [66] J. Duan and P. Holmes, *Nonlinear Anal.* **22**, 1033 (1994).
- [67] J. Duan, P. Holmes, and E. S. Titi, *Nonlinearity* **5**, 1303 (1992).
- [68] S. Bottin and J. Lega, *Eur. Phys. J. B* **5**, 299 (1998).
- [69] H. Riecke, *Physica D* **92**, 69 (1996).
- [70] H. Riecke, *Phys. D (Amsterdam, Neth.)* **61**, 253 (1992).
- [71] W. Barten, M. Lücke, M. Kamps, and R. Schmitz, *Phys. Rev. E* **51**, 5662 (1995).
- [72] M. Lücke, W. Barten, and M. Kamps, *Phys. D (Amsterdam, Neth.)* **61**, 183 (1992).
- [73] P. Kolodner, *Phys. Rev. A* **46**, 6431 (1992).
- [74] N. Akhmediev and J. M. Soto-Crespo, *Phys. Rev. E* **70**, 036613 (2004).
- [75] J. Burke and E. Knobloch, *Chaos* **17**, 037102 (2007).
- [76] J. A. Sherratt and M. J. Smith, *Phys. D (Amsterdam, Neth.)* **241**, 1671 (2012).
- [77] D. Urzagasti, D. Laroze, and H. Pleiner, *Eur. Phys. J.: Spec. Top.* **223**, 141 (2014).
- [78] J. D. Scheel and M. C. Cross, *Phys. Rev. E* **74**, 066301 (2006).
- [79] A. Karimi and M. R. Paul, *Phys. Rev. E* **85**, 046201 (2012).
- [80] D. Laroze, J. Bragard, O. J. Suarez, and H. Pleiner, *IEEE Trans. Magn.* **47**, 3032 (2011).
- [81] D. Laroze, P. G. Siddheshwar, and H. Pleiner, *Commun. Nonlinear Sci. Numer. Simul.* **18**, 2436 (2013).
- [82] C. Bonatto and J. A. C. Gallas, *Phys. Rev. Lett.* **101**, 054101 (2008).
- [83] L. Nana, A. B. Ezersky, N. Abcha, and I. Mutabazi, *J. Phys.: Conf. Ser.* **137**, 012006 (2008).
- [84] M. G. Clerc and N. Verschueren, *Phys. Rev. E* **88**, 052916 (2013).
- [85] Li Hai-Hong, X. Jing-Hua, H. Gang, and H. Bambi, *Chin. Phys. B* **19**, 050516 (2010).